JGR Biogeosciences

RESEARCH ARTICLE
10.1029/2025JG008922

Year-Round $\delta^{13}C$-CH_4 Reveals Seasonal Transition in Methane-Related Processes in a Boreal Mire

Xuefei Li[1], Janne Rinne[2], Eeva-Stiina Tuittila[3], and Timo Vesala[1,4]

[1]Institute for Atmospheric and Earth System Research (INAR)/Physics, Faculty of Science, University of Helsinki, Helsinki, Finland, [2]Natural Resources Institute Finland, Helsinki, Finland, [3]University of Eastern Finland, Joensuu, Finland, [4]Institute for Atmospheric and Earth System Research (INAR)/Forest Sciences, Faculty of Agriculture and Forestry, University of Helsinki, Helsinki, Finland

Key Points:

- Unique year-round in situ data set of $\delta^{13}C$-CH_4 and [CH_4] in peat water and in emitted CH_4 revealed seasonal dynamics of CH_4 processes
- We found reversal profiles of $\delta^{13}C$-CH_4 in peat water between summer and winter
- Seasonal changes in the dominant CH_4 transport pathways were indicated by the differences in $\delta^{13}C$ in emitted CH_4 and in peat water

Supporting Information:

Supporting Information may be found in the online version of this article.

Correspondence to:

X. Li,
xuefei.z.li@helsinki.fi

Citation:

Li, X., Rinne, J., Tuittila, E.-S., & Vesala, T. (2025). Year-round $\delta^{13}C$-CH_4 reveals seasonal transition in methane-related processes in a boreal mire. *Journal of Geophysical Research: Biogeosciences*, *130*, e2025JG008922. https://doi.org/10.1029/2025JG008922

Received 14 MAR 2025
Accepted 3 SEP 2025

Author Contributions:

Conceptualization: Xuefei Li, Janne Rinne
Data curation: Xuefei Li
Formal analysis: Xuefei Li, Janne Rinne
Funding acquisition: Xuefei Li, Timo Vesala
Investigation: Xuefei Li, Janne Rinne
Resources: Eeva-Stiina Tuittila
Supervision: Eeva-Stiina Tuittila, Timo Vesala
Writing – original draft: Xuefei Li, Janne Rinne
Writing – review & editing: Xuefei Li, Janne Rinne, Eeva-Stiina Tuittila, Timo Vesala

Abstract While boreal mires are known to be a significant natural source of methane (CH_4), the seasonality of the related processes and their controls are still poorly understood. Here we aim to characterize CH_4 production, oxidation and transport, and their drivers in a boreal mire using year-round continuous measurements of stable carbon isotope composition ($\delta^{13}C$-CH_4) in dissolved and emitted CH_4. We found reversed vertical profiles of $\delta^{13}C$-CH_4 in the summer (higher values at surface) and in the winter (higher values at bottom). The ^{13}C enriched emitted CH_4, as compared to pore water CH_4, indicated methane oxidation at the peat-snow interface by sphagnum mosses in the winter. The observed hysteretic $\delta^{13}C$-CH_4 - pCH_4 relation indicated the importance of substrate availability for methane production in addition to soil temperature, and their time-lagged seasonal cycles. Our data also demonstrated the dominance of plant-mediated transport in the summer, the dominance of diffusion through peat and moss matrix (with associated microbial methane oxidation) in the winter and a transition in the spring and autumn. In general, the measured $\delta^{13}C$ values of emitted CH_4 at this and other northern mires are considerably lower than the values used in atmospheric inversion models. Our comprehensive data set provided invaluable insight into wetland $\delta^{13}C$-CH_4, the dynamic interplay of multiple processes related to CH_4 emission in boreal mires, especially in the rarely studied winter, spring, and autumn, the incorporation of which into Earth System Models will allow more accurate prediction of wetland responses to ongoing climate change.

Plain Language Summary Northern mires emit significant amounts of methane, a potent greenhouse gas, which vary seasonally and are influenced by the changing climate. In this study, we aim to evaluate stable carbon isotope ^{13}C abundancies in emitted methane and its seasonal variations in a boreal mire, as well as the temporal interplay of the methane-related processes through a continuous in situ measurement. Our data revealed the dominance of methane production over oxidation for most of the year, except in winter. For the first time, we observed the reversal of vertical profiles of $\delta^{13}C$ in dissolved methane between winter and summer, which resembled the methane geochemistry commonly considered from different types of mires. Our data supported seasonal differences in the dominant transport pathways, with methane being transported through vascular plants in the growing season and through the peat matrix in winter. We showed the time lag between the main drivers of methane production, peat temperature, and substrate availability. In the end, we observed overall lower values of $\delta^{13}C$ in the emitted methane compared to those used in atmospheric inversions. The systematic error of wetland $\delta^{13}C$ in the global methane model is likely to lead to a considerable bias in methane source apportionment.

1. Introduction

Boreal mires (i.e., natural peatlands) are significant natural sources of methane (CH_4), one of the major greenhouse gases, into the atmosphere (Ciais et al., 2013). The emission of CH_4 from these ecosystems depends on the temporal variations of environmental variables (e.g., Rinne et al., 2007), spatial extent of the mires (e.g., Peltola et al., 2019), and on complex interactions between climatic and biogeochemical characteristics (Turetsky et al., 2014). The net emission of CH_4 from a wetland ecosystem is a result of CH_4 production, CH_4 oxidation, and CH_4 transport processes (Chanton, 2005; Lai, 2009). As the changing climate can affect the CH_4 emission from wetlands, potentially leading to climate feedback effects (Gedney et al., 2004; Zhang et al., 2023), understanding the processes behind the CH_4 emission from wetland systems is crucial.

CH_4 in wetlands is produced by *Archaea* via different pathways mainly depending on substrate availability and temperature (Schulz et al., 1997). CH_4 produced via hydrogenotrophic methanogenesis (HM) is more depleted in ^{13}C than produced via acetoclastic methanogenesis (AM) (Hornibrook, 2009; McCalley et al., 2014; Whiticar et al., 1986). $^{12}CH_4$ is preferentially consumed during CH_4 oxidation so that the residual CH_4 becomes ^{13}C-enriched (Hornibrook, 2009; Whiticar, 1999). In addition, molecular diffusion also causes isotopic fractionation, as $^{12}CH_4$ molecule has a faster translational velocity than $^{13}CH_4$ due to their mass difference. The preferential loss of $^{12}CH_4$ results in $^{13}CH_4$-enrichment in the residual CH_4 pool during the transport of CH_4 via plant aerenchyma, a form of diffusive transport mainly bypassing CH_4 oxidation. CH_4 transport via ebullition (bubbles) involves no or very low isotopic fractionation due to the fast movement of gas (Chanton, 2005). Thus, natural stable isotope abundances in dissolved and emitted CH_4, commonly expressed as $\delta^{13}C$-CH_4 values, offered additional constraints for our understanding of the processes underlying CH_4 emission from ecosystems.

While the CH_4 emissions from boreal mires exhibit systematic seasonal variability, with high emission rates during growing season (GS) and lower rates in non-growing season (NGS) (Heiskanen et al., 2021; Keane et al., 2021; Rinne et al., 2018; Riutta et al., 2007), the $\delta^{13}C$ values of emitted CH_4 show less systematic temporal variability (McCalley et al., 2014; Rinne et al., 2022). The inconsistency can be attributed to the occurrence of the underlying CH_4 processes that have different temporal patterns. Investigation of pore water $\delta^{13}C$ values along a vertical gradient can provide a better insight into the separation of these processes, as it is close to where CH_4 is produced. There is typically a vertical gradient in the $\delta^{13}C$-CH_4 values along the peat profiles in mires, but the pattern is different between the mire types (Hornibrook, 2009). In sedge dominated fens, the pore water CH_4 is generally less depleted in ^{13}C than in moss and dwarf shrub dominated bogs and their $\delta^{13}C$ values are the lowest in deeper peat layers. This has been interpreted as an indication of acetoclastic methane production in shallower layers, where the majority of substrate-providing vascular plant roots are located, and increasingly HM in deeper peat layers. Contrastingly, in bogs with generally very ^{13}C-depleted CH_4 indicating the dominance of HM, $\delta^{13}C$-CH_4 values are the lowest near the surface.

A static temperature function of CH_4 production and/or CH_4 emission has been prescribed in many terrestrial biogeochemical models (Wania et al., 2013; Xu et al., 2016). Although such static temperature-dependency has been supported by meta-analyses across microbial to ecosystem scales (Yvon-Durocher et al., 2014), the hysteretic responses of CH_4 emission to the seasonal cycles of vegetation processes providing substrates for methanogenesis (Rinne et al., 2018) and of temperature (Chang et al., 2021) have been observed from boreal mires, that is, peat forming wetlands, suggesting that both substrate and temperature control wetland CH_4 emissions and they have time-lagged seasonal cycles (Chang et al., 2020). The application of isotopic methods with novel online measurement tools with high temporal resolution are useful in characterizing the importance of these two controls (Rinne et al., 2022; Sabrekov et al., 2024).

The understanding on the seasonal cycle of $\delta^{13}C$-CH_4 dissolved in pore water, its coupling with $\delta^{13}C$ in the emitted CH_4, and their implications to the CH_4 production, oxidation and transport processes in the peat is very limited. Previously, in situ $\delta^{13}C$-CH_4 in pore water and in emitted CH_4 were either studied separately (Heiskanen et al., 2021; Sabrekov et al., 2024), or they were studied simultaneously but with coarse temporal resolution (Kuhn et al., 2024; McCalley et al., 2014). Besides, most of the data on $\delta^{13}C$-CH_4 and CH_4 concentrations in pore water (expressed as equilibrium partial pressure, pCH_4) have been collected in a non-continuous manner (mostly in the GS), thus yielding only snapshots but not the temporal development (Knorr et al., 2008; Shoemaker & Schrag, 2010). There are likely to be drastic seasonal changes in for example, the input of fresh root exudates and oxygen into the peat following the phenological status of aerenchymatous sedges, especially in early GS and during their senescence. Furthermore, in boreal mires, snow and ice cover the peat from the atmosphere for several months, during which relatively small but systematic emissions of methane into the atmosphere have been observed (Dise, 1992; Heiskanen et al., 2021; Rinne et al., 2018).

Here we conducted the first year-round vertical peat profile measurements of pCH_4 and $\delta^{13}C$-CH_4 in pore water, and we inversely calculated ecosystem-scale $\delta^{13}C$-CH_4 (integrated over a large area) in the emitted methane using nocturnal boundary-layer accumulation approach (see Section 2.3) in a boreal mire. We aimed (a) to evaluate the $\delta^{13}C$ values of emitted and pore water CH_4, and the seasonality of those values from a boreal mire, (b) to infer the temporal development of methanogenesis, methanotrophy and methane transport as well as their controls using $\delta^{13}C$-CH_4 data as proxy, and (c) to explain the potential time-lags between them. We asked the following questions: (Q1) How do CH_4 production, oxidation along a vertical profile and CH_4 transport pathways vary over

a full annual cycle in a boreal mire? (Q2) How do soil temperature and substrate availability drive the seasonal cycle of pore water pCH_4?

To answer Q2, we adapted the conceptual framework proposed by Rinne et al. (2022) and formulated two parallel hypotheses which were to be evaluated by the observed relationships between pore water $\delta^{13}C\text{-}CH_4$ and pCH_4 (Figure A1). A possible negative correlation between pCH_4 and $\delta^{13}C\text{-}CH_4$ would indicate CH_4 oxidation mainly drives the pCH_4 variation because the enzymatic reaction of CH_4 oxidation typically consume preferably $^{12}CH_4$ leading to a ^{13}C enrichment in the residual pore water CH_4 along with a reduction of pCH_4. Conversely, a possible positive correlation between pCH_4 and $\delta^{13}C\text{-}CH_4$ would indicate the dominance of CH_4 production over CH_4 oxidation driving the pCH_4, as has been demonstrated during thawed periods in previous studies (Chang et al., 2020; Kuhn et al., 2024; McCalley et al., 2014). Higher $\delta^{13}C\text{-}CH_4$ is usually associated with CH_4 productions with better substrate availability for methanogenesis from more productive mires (Chanton et al., 2005). The better substrate condition can be higher acetate concentration or higher H_2 concentration, which indirectly influence $\delta^{13}C$ through the energetics of hydrogenotrophic methane production (Hornibrook, 2009), thus the change in $\delta^{13}C\text{-}CH_4$ does not necessarily imply changes in methane production pathways.

2. Materials and Methods

2.1. Site Description

The study was conducted from 16 March 2022 to 15 March 2023 in a boreal mire (61°49.961′N, 24°11.567′E, 160 m a.s.l.) within the large Siikaneva mire complex in Ruovesi, southern Finland, located in the south boreal zone (Rinne et al., 2007). The site has a relatively flat topography and vegetation is dominated by sedges (*Carex rostrata*, *C. limosa*, *Eriophorum vaginatum*, *Scheuchzeria palustris L.*) and *Sphagnum* mosses (Riutta et al., 2007). The annual mean temperature was 4.1°C and the annual precipitation was 690 mm during 1991–2020 (Jokinen et al., 2021). The GS (between the first 5-day period with average temperatures above 5°C and the first 5-day period with average temperatures below 5°C) of the site is usually between the end of April and mid-October (Finnish Meteorological Institute, 2024). The peat depth at the measurement site is about 4 m (Mathijssen et al., 2016). The pH of the site varies between 4.4 and 4.7 along the peat profile. The site is a Class 2 ecosystem station *FI-Sii* of ICOS Research Infrastructure (Heiskanen et al., 2022). The mire complex is surrounded mostly by forest and there are no anthropogenic methane sources (Figure 1a).

2.2. Automatic Measurement of Pore Water pCH_4 and $\delta^{13}C\text{-}CH_4$

For the continuous measurement of pore water pCH_4 and $\delta^{13}C\text{-}CH_4$ profile, three 50 m long tubes (19 mm OD, 16 mm ID) made of Teflon, referred to as sample tubes in the following text, were installed in the peat at depths of 10, 30, and 50 cm below the peat surface in 2013 (Figures 1b and 1c). The total internal volume of each sample tube was circa 2.5 L. The sample tubes were connected to a cavity ring-down spectrometer (CRDS; Picarro G2201-I, Picarro Inc., Santa Clara, USA) by a four-way valve. The air in the tubes was allowed to equilibrate with pore water for 45 hr, before pumping it through the analyzer, while a venting tube in the other end of the sample tubes allowed ambient air to replace the air in the sample tubes. The time required for equilibration was selected based on a laboratory test (Figure S1 in Supporting Information S1). As the mixing ratios in the sample tubes far exceeded the analyzer range, 1:99 dilution with ambient air was applied by a dedicated dilution system. Average CH_4 mixing ratios (and pCH_4) and its standard deviation, measured in the ambient air 40 cm above the mire surface during the sampling, were 1.96 ± 0.06 ppm (0.195 Pa),1.97 ± 0.05 ppm (0.196 Pa), and 2.04 ± 0.22 ppm (0.203 Pa) at 12–15, 15–18, and 18–21 hr, respectively (Figure S2 in Supporting Information S1). The time windows correspond to the times of measurement from the depths of 10, 30, and 50 cm, respectively. As there were no significant differences between the time intervals, we used the mean CH_4 concentration from the background ambient air (1.99 ppm) in Equation B1 to calculate CH_4 concentrations in the peat water and Equation B2 to calculate the $\delta^{13}C\text{-}CH_4$ values. In most cases the uncertainty caused by the 1:99 dilution with ambient air was less than 3% for pCH_4, and less than 7% in the extremely low mixing ratio in the sampling tube . The uncertainty in the $\delta^{13}C\text{-}CH_4$ caused by the dilution was in most cases below 1‰ units, and even in the extreme cases below 3‰ units. Calculation of dilution effects is presented in Appendix B. The methane concentration is expressed in methane partial pressure (pCH_4) both in gaseous and in dissolved form. An average atmospheric pressure during the measurement period of 99.2 kPa was used in the calculation. In order to compare with other studies and to incorporate the influence of temperature on solubility in the reported CH_4

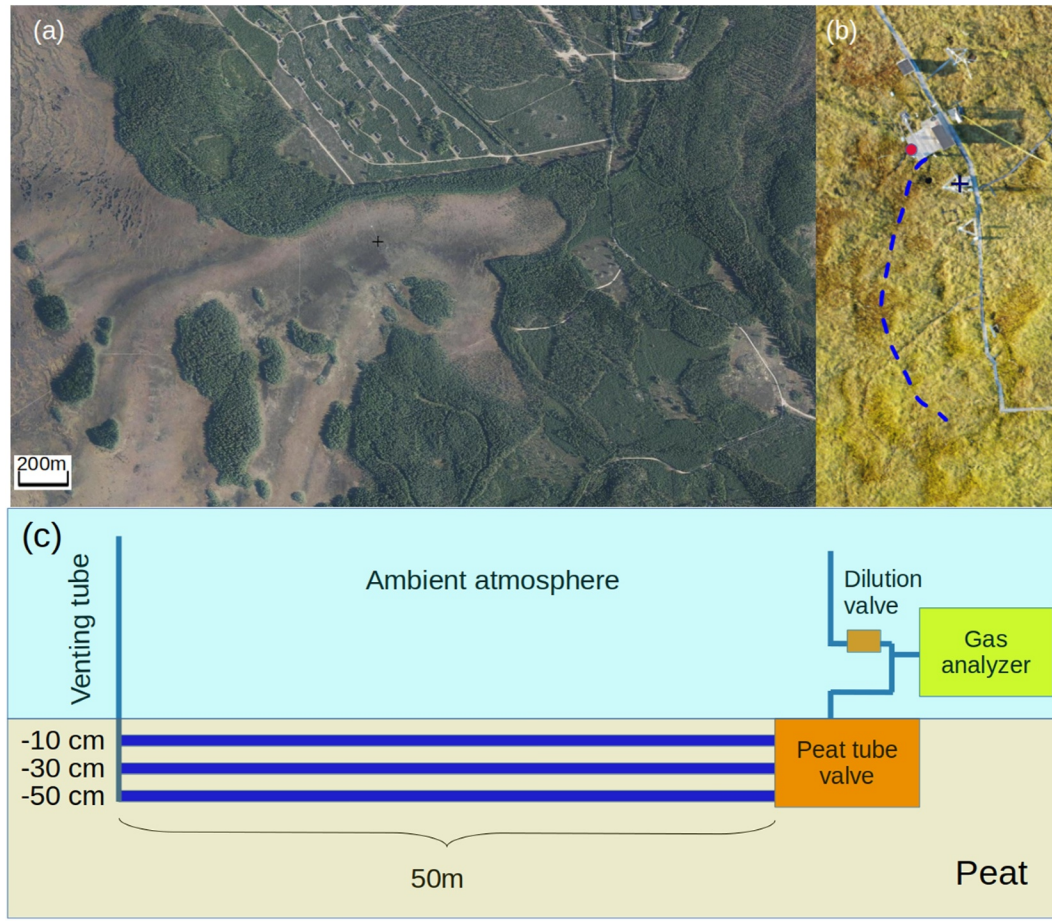

Figure 1. Aerial pictures of the study area and measurement design. (a) Aerial picture of the surrounding landscape of the field site. (b) A close-up of the measurement site from an aerial picture. There are no anthropogenic methane sources, such as cattle farms or gas pipelines, in the vicinity of the mire. Cross indicates the location of the eddy covariance tower. The red dot shows the inlet for an ambient atmosphere. The blue dash line shows the locations of the soil tubes. (c) Schematic of the measurement system.

concentrations, we convert the methane concentration to μmol L^{-1} using temperature-dependent Henry's law constant and report them in Supporting Information S1.

2.3. Automatic Measurement of Methane Emissions and $\delta^{13}C$ in Emitted CH_4

The ecosystem level CH_4 flux continuously measured in the study site according to ICOS protocols by the eddy covariance method (Nemitz et al., 2018) was used to derive daily average methane fluxes during the measurement period.

The ecosystem-scale $\delta^{13}C$ values of the emitted CH_4 was obtained using nocturnal boundary-layer accumulation approach (Quay et al., 1988). The measurements of atmospheric surface layer CH_4 mixing ratios and corresponding surface layer $\delta^{13}C$-CH_4 values were conducted every second night (when gas from the sample tubes was not measured) by drawing ambient air from 0.4 m above the peat surface to the CRDS analyzer. To estimate concentration and flux source areas footprint models of varying complexity are commonly used. We ran a Lagrangian stochastic transport model for flux and concentration footprints (Rannik et al., 2003) using different surface layer stabilities and roughness lengths to obtain the footprint of the measured surface layer CH_4 concentration and CH_4 flux at different conditions. For our measurement height, the cumulative 80% flux footprint was between 3.9 and 9.4 m (Table S1 in Supporting Information S1). The cumulative footprint distances for concentration could not be defined as there was no saturation of these functions even with a simulation domain of 1km. Since the concentration footprint is typically at least an order of magnitude larger than the flux footprint, the

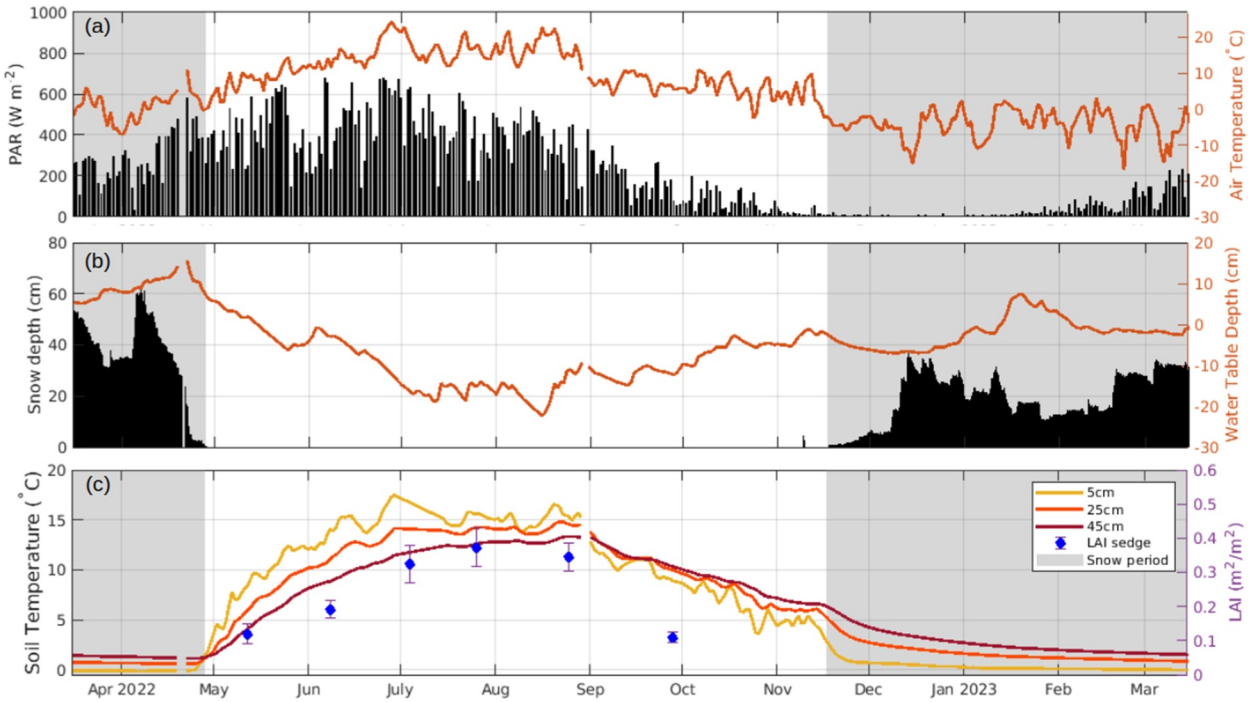

Figure 2. General annual cycle of environmental parameters: daily average of (a) PAR and air temperature, (b) snow depth and water table depth, and (c) soil temperature at 5, 25, and 45 cm belowground and leaf area index (LAI) of sedges. In panel (c), solid dots represented the mean LAI of sedges from 15 subplots and error bars denoted the standard error of the mean. The snow period is shaded in light gray.

measured CH_4 concentration and $\delta^{13}C$-CH_4 signals are likely originating from distances up to 100 m or more from the observation location.

We calculated the zenith angle of the sun at the site and time periods when the zenith angle was greater than 90° were considered as nighttime. The $\delta^{13}C$ values of the emitted methane were then obtained by the Keeling plot approach (Keeling, 1958) separately for each night. To reduce the uncertainty of $\delta^{13}C$-CH_4 due to the low range of measured CH_4 mixing ratios, occurring especially during winter nights, only Keeling plots with R-square greater than 0.8 were used in the further analysis, leading to 17.2% of the Keeling plots to be discarded.

2.4. Axillary Manual Measurements of Environmental Variables

Leaf area index (LAI, m^2/m^2) of all plants, sedge and shrub were measured from 15 sample plots in the study area throughout the GS on 12 May, 8 June, 4 July, 26 July, 25 August, and 28 September 2022. The sampling method was detailed in Korrensalo et al. (2018). Briefly, we set up five 8 × 8 cm subplots within each of the sample plots, counted the number of green leaves in each subplot and measured the average leaf size with a scanner. Only LAI of sedge is reported in the results. Manual pore water samples were collected from the study site in July 2022. Samples were filtered upon collection and transported to the lab immediately in a cool box and analyzed for different components with ion chromatography at the University of Vienna. All statistical analyses were conducted in MATLAB (MathWorks, Inc., Natick, MA, USA).

3. Results

3.1. Environmental Condition During the Study Period

Over the study period from 16 March 2022 to 15 March 2023, the average daily air temperature ranged from −16.9°C (22 February 2023) to 24.3°C (28 June 2022), with an annual mean temperature of 4.8°C (Figure 2a). The snow-free period lasted six and half months from the end of April to the middle of November 2022. The deepest snow depth (~60 cm) occurred in early April. The GS started on 24 April 2023 and ended on 19 October 2023.

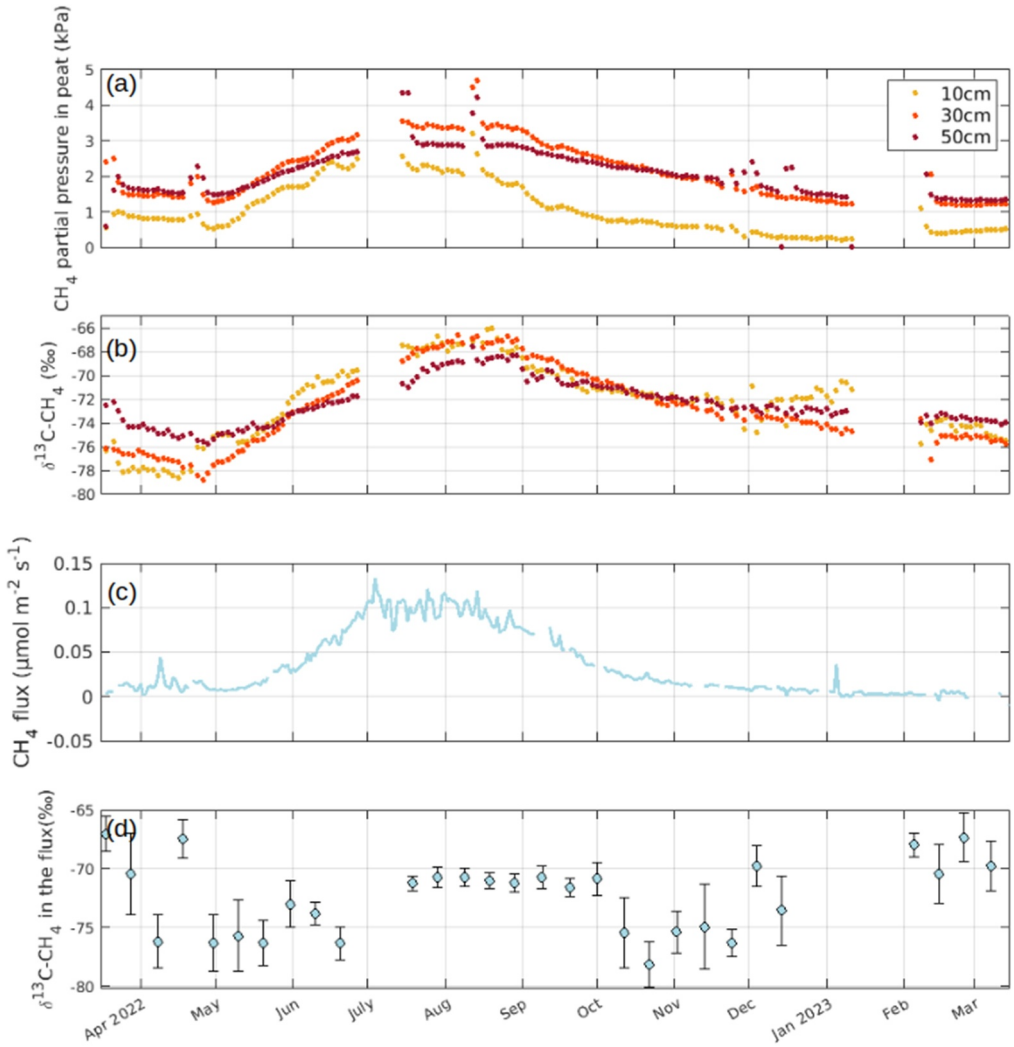

Figure 3. Annual cycle of (a) dissolved methane expressed as methane partial pressure (pCH_4), (b) $\delta^{13}C$ value of dissolved methane at 10, 30, and 50 cm belowground, (c) methane flux as measured by the eddy covariance system, and (d) $\delta^{13}C$ value of emitted CH_4 as measured by the nocturnal boundary-layer accumulation approach.

Water table (WT) that ranged between 15.6 cm above and 22.3 cm below peat surface had its maximum in the spring during the snow melt period, after which it declined toward the end of the summer. Between 25 June and 30 September 2022, the WT was at about −10 cm or lower, indicating the peat tube at −10 cm was not fully submerged in water (Figure 2b). Average peat temperature at 5, 25, and 45 cm below the peat surface was 6.0°C, 6.2°C, and 6.2°C over the entire studied year, 0.2°C, 1.2°C, and 2.0°C during snow-covered period and 10.9°C, 10.3°C, and 9.5°C during snow-free period.

The average LAI of sedges (LAI_{sedge}) during the snow-free period was 0.24 ± 0.02 m^2/m^2 and peaked at the end of July at 0.37 ± 0.05 m^2/m^2 (Figure 2c). In the spring (from end of April to mid-June) and in the autumn (from September to mid-November), LAI_{sedge} were ca. 0.1 m^2/m^2.

3.2. pCH_4, CH_4 flux, $\delta^{13}C$ in Pore Water and Emitted CH_4

The pCH_4 in the peat exhibited a clear annual cycle at all three measurement depths (−10, −30, and −50 cm), with the highest values between July and August, corresponding to the highest air and peat temperatures and highest CH_4 emission (Figure 3a and Figure S3 in Supporting Information S1). During the snow-covered period, pCH_4 levels were generally low, and had an increasing trend with increasing peat depth. With the start of the snow-free period in May, pCH_4 rapidly increased at all peat depths, especially at the two top depths where peat temperature

similarly increased. pCH_4 was the highest at −30 cm between mid-May and end of October, followed by that at −50 and −10 cm. At −10 cm, pCH_4 was lower than at deeper depths during the whole annual cycle. There was a short-term increase of pCH_4 at all peat depths during the spring thawing period in April. Over an annual cycle, pCH_4 at different depths ranged from 0.22 to 3.2 kPa, from 1.19 to 5.82 kPa, and from 1.31 to 4.33 kPa at −10, −30, and −50 cm, respectively.

The $\delta^{13}C\text{-}CH_4$ in the peat profile also demonstrated an annual cycle with relatively low values during snow-covered winter period and relatively high values in summer (Figure 3b). At all peat depths there was a decreasing trend of $\delta^{13}C\text{-}CH_4$ as winter proceeded. As the snow-free period began at the end of April, $\delta^{13}C\text{-}CH_4$ values started to increase. Interestingly, along the soil profile CH_4 at deeper peat were more enriched with ^{13}C at winter, while a clearly inversed pattern was observed in summer, with CH_4 at deepest peat layer being most ^{13}C depleted. The two cross-over periods, where similar $\delta^{13}C\text{-}CH_4$ values appeared at all the depths, were in the second half of May and in the second half of October. With the onset of snow cover in December 2022, $\delta^{13}C\text{-}CH_4$ values at −10 cm remained constant while those values from deeper peat became progressively more negative.

Characteristic to most boreal mires, ecosystem level CH_4 emission exhibited strong seasonal variation during the studied period with the highest values in July 2022 (Figure 3c). The highest daily average emission appeared in July 2022 (0.134 μmol m^{-2} s^{-1}). During the snow-covered period CH_4 flux was generally low but non-zero. From December 2022 to the end of March 2023, the monthly average of CH_4 flux ranged between 0.002 and 0.008 μmol m^{-2} s^{-1}. There was a smaller CH_4 emission peak during the spring thawing in April 2023, with the highest daily value reaching 0.044 μmol m^{-2} s^{-1}.

Ten-day averages of $\delta^{13}C$ in the emitted CH_4, derived using the nocturnal boundary-layer accumulation approach, showed seasonal variation (Figure 3d). $\delta^{13}C$ values of the emitted CH_4 were relatively stable from July to September 2022 with an average value of −72.8‰. During the winter snow-covered period (from March to mid-April 2022, December 2022 to mid-March 2023), $\delta^{13}C\text{-}CH_4$ was on average −70.0‰. The emitted CH_4 was more depleted in ^{13}C in the spring and autumn, with average $\delta^{13}C\text{-}CH_4$ values being −75.3‰ in the spring and −76.1‰ in the autumn.

3.3. Relationships Between $\delta^{13}C\text{-}CH_4$, pCH_4, and CH_4 Flux

Daily pCH_4 and $\delta^{13}C\text{-}CH_4$ in pore water were positively correlated with each other, both having higher values at all depths in summer and lower values in winter (−30 cm as in Figure 4a; $R^2 = 0.59$, $p < 0.001$). There was hysteresis-like behavior (i.e., time-lag) in the correlation, with $\delta^{13}C\text{-}CH_4$ values at the same pCH_4 level in the early season being lower than in the late season.

The 10-day averages of $\delta^{13}C$ in emitted CH_4 and 10-day averages of CH_4 fluxes during the snow-free period had positive correlation (Figure 4b; $R^2 = 0.59$, $p < 0.001$). Similarly to pore water $pCH_4 - \delta^{13}C\text{-}CH_4$, the relationship showed hysteresis-like behavior with data points from early season (approximately from May to August) occupying the lower right space in the plot and late season (approximately from August to October) the upper left space, which formed a circle in the data space.

The comparison between 10-day averages of $\delta^{13}C\text{-}CH_4$ in pore water and that in emitted CH_4 demonstrated that the dominant CH_4 transport pathways varied seasonally (Figure 4c). During the peak GS when soil temperature at 25 cm (Ts_{-25}) ranged from 12.1°C to 14.5°C, $\delta^{13}C$ values in emitted CH_4 were lower than those in pore water (Figure 4c, below 1:1 line). Conversely, during winter time when Ts_{-25} was between 0.6°C and 1.1°C, $\delta^{13}C$ values in emitted CH_4 were higher than those in pore water (Figure 4c, above 1:1 line). When Ts_{-25} was between 3.9°C and 9.5°C, the data points were located at both sides of the 1:1 line.

4. Discussion

The pCH_4 in the pore water in the uppermost 50 cm peat profile shows up to four orders of magnitude higher values than in the atmosphere, indicating a gradient driving the emission from the peat into the atmosphere throughout the year. During and around the snow-free period, from May to October, the highest pCH_4 values were observed at the depth of 30 cm, indicating that this is the likely depth range for methanogenesis due to the substrate input by root systems of vascular plants (Korrensalo et al., 2017). This is also in line with the observation of the ecosystem level methane emissions at this site being best correlated with the temperature at the depths of

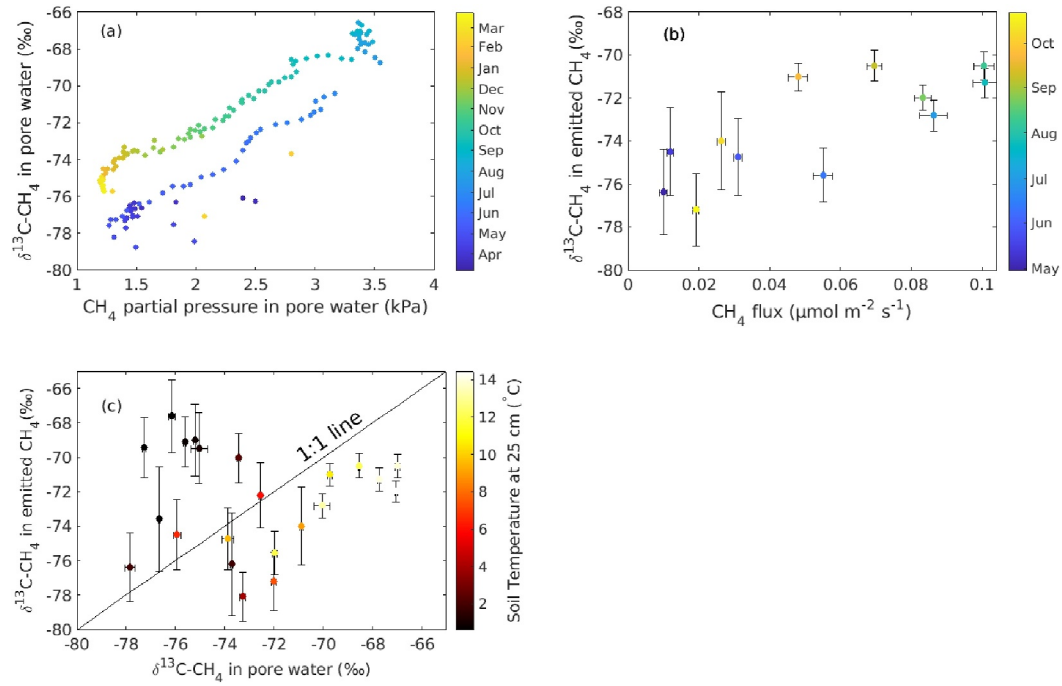

Figure 4. (a) δ^{13}C-CH_4 against CH_4 partial pressure in pore water at 30 cm belowground. (b) Ten-day averages of δ^{13}C-CH_4 in emitted CH_4 against 10-day average of CH_4 fluxes during the snow-free period. In panels (a, b), the color bar indicates the time of the year. (c) Ten-day average of δ^{13}C-CH_4 in emitted CH_4 against δ^{13}C-CH_4 in pore water at 30 cm. In panel (c), the error bars show standard error of the mean and the color bar indicates 10-day average soil temperature at 25 cm belowground. The diagonal line represents 1:1 relationship between δ^{13}C-CH_4 in emitted CH_4 and in the pore water, corresponding to the absence of fractionation during CH_4 transport from the pore water to the atmosphere, for example, ebullition. The data points below the 1:1 line indicate the domination of CH_4 transport through diffusive plant-mediated transport, while the data points above the 1:1 line indicate CH_4 transport by diffusion through peat and moss matrix, with associated microbial CH_4 consumption.

around 30 cm (Rinne et al., 2007, 2018). During the winter months the pCH_4 increases monotonically with depth, leading to an upward diffusion of CH_4 throughout the peat layer.

The annual cycle of the δ^{13}C-CH_4 in the pore water at all depths showed a distinct pattern. The start of the period with increase of δ^{13}C-CH_4 values and pCH_4 in spring coincides with the spring thaw and increasing peat temperatures. The δ^{13}C-CH_4 values and pCH_4 start rising simultaneously and eventually reached their maximum values in the main rooting depth of sedges (Figures 3a and 3b), indicating methanogenesis, rather than methanotrophy, is the main controlling process for the CH_4 concentration in the peat during the GS, as also suggested in previous studies (Chang et al., 2020; Kuhn et al., 2024; McCalley et al., 2014).

The observed summertime vertical δ^{13}C-CH_4 profile in the peat was typical for fen (minerotrophic mire), with the lowest values in deeper peat and highest values near the surface (Hornibrook, 2009). This phenomenon aligns with our expectations and those of previous studies. It has been conventionally associated with the predominance of AM in the shallow peat, where ample root exudate provides acetic acids for the methanogens, while the more ^{13}C-depleted CH_4 at the bottom has been interpreted as a transition to HM due to the lower temperature and lack of labile substrate (Hornibrook et al., 1997; Popp et al., 1999).

By contrast, the inverted wintertime δ^{13}C-CH_4 profile (lower δ^{13}C values at the surface and higher δ^{13}C values at the bottom) is surprising and yet to be explained. First, such a profile resembles those observed in ombrotrophic bogs, where the lower δ^{13}C-CH_4 values have been attributed to the prevalence of HM due to the low temperature and a lack of labile substrate (Hornibrook, 2009; Whiticar et al., 1986). The wintertime profile could result from a shift from AM to HM. However, we are lacking data on the co-existing isotope species such as δ^{13}C-CO_2, ^{2}H-CH_4 that we cannot determine the methanogenic pathways conclusively. Second, the soil temperature profile in the winter could also influence δ^{13}C-CH_4, as higher soil temperature in deeper layers

could lead to a smaller CO_2-CH_4 fractionation (so that CH_4 is δ^{13}C-enriched). But such a temperature effect would have been very small at our site, if applicable. It has been reported that the isotopic fractionation decreases by 60‰ over a temperature increase of 110°C (Whiticar et al., 1986). At our site, the average winter soil temperature in 2022 was −0.1°C, 0.7°C, and 1.3°C at 5, 25, and 45 cm, respectively. The ca. 1°C temperature difference between the surface and the bottom layers would have resulted in only less than 0.6‰ difference in fractionation, assuming the temperature dependence was linear. In conclusion, the relative importance of the mechanisms behind the wintertime δ^{13}C-CH_4 profile remains unclear. Studies targeting both carbon and hydrogen isotopes in emitted and porewater CH_4, and those using stable carbon isotope tracers to quantify the relative rates of acetoclastic and HM are highly valued.

The variations of δ^{13}C in emitted CH_4 did not seem to fully follow the δ^{13}C-CH_4 in the pore water. However, its temporal variation appeared to be symmetrical with the middle part in the peak GS (Figure 3d). δ^{13}C-CH_4 in the emitted CH_4 was relatively high (mean value as −70.0‰) during the winter (March–mid-April 2022, January–March 2023), considering the ^{13}C-depleted CH_4 of the surface pore water (mean value −75.2‰, Figure 3b). To our knowledge, this phenomenon has never been observed before. It could be explained by CH_4 oxidation at the peat-snow interface by methanotrophs on sphagnum mosses, as ^{12}C is preferentially consumed during oxidation, leading to ^{13}C enriched residual CH_4 being emitted (Hornibrook, 2009). After the snow melting, vascular plants appeared, facilitating CH_4 transport via aerenchyma and resulting in lower δ^{13}C-CH_4 in the emitted CH_4, as methanotrophy is thus bypassed. Low δ^{13}C-values of emitted CH_4 in the beginning of the summer season have also been observed by Perryman et al. (2024). After the end of the peak GS, highly efficient plant-mediated CH_4 transport continues through the aerenchyma of senesced peatland sedges, as demonstrated by the plant-removal experiment conducted in the same peatland complex (Jentzsch et al., 2024). During the peak GS, the emitted CH_4 was more ^{13}C enriched (on average −71.0‰) compared to the spring before it (on average −75.3‰) and the autumn after it (on average −76.1‰), which can be mainly attributed to the ^{13}C enriched CH_4 in the surface pore water (Figure 3b) due to the abundant root exudate as substrate for methanogens.

Generally, the observed pCH_4 and δ^{13}C-CH_4 in peat water show a positive correlation (Figure 4a), indicating that it was mostly CH_4 production, rather than CH_4 oxidation, contributing to the pore water δ^{13}C-CH_4 on an annual scale in the boreal mire. In the wintertime the relationship between pCH_4 and δ^{13}C-CH_4 in the peat water was not clear (Figure 4a), which may indicate the importance of oxidation during NGS when CH_4 production is weak. Previous studies demonstrated time-lagged temperature effects on CH_4 emission, suggesting that such phenomenon may be due to the elevated methanogen biomass and activity driven by substrate availability at the late season (Chang et al., 2020, 2021). In our study, the hysteresis-like behavior between pCH_4 and δ^{13}C-CH_4 indicated that substrate availability plays a considerable role in the seasonal cycle of the CH_4 emission and there was a time-lag in the seasonal cycles of substrate availability and CH_4 production (HS 2.2). Similar behavior was also observed for relation between δ^{13}C in emitted CH_4 and CH_4 emission rate (Figure 4b) and in a previous study (Rinne et al., 2022). Thus, the annual cycle of methane emission is a product of both temperature dependent metabolism of methanogenic Archaea and the availability of substrates for methanogenesis, both indicating time-lagged behavior in relation to surface temperature.

The relation of δ^{13}C-CH_4 in pore water versus δ^{13}C in emitted CH_4 revealed seasonal changes in the transport pathways of CH_4 from peat into the atmosphere (Figure 4c). Since we used 10-day averaged data, it is hard to evaluate ebullition as a transport pathway due to its sporadic nature. Rather, the presented data is a net balance from multiple processes and sheds light on the dominant CH_4 transport pathway over 10 days. During the summertime, as indicated by peat temperature, the data at Siikaneva falls below the 1:1 line. This indicated that diffusive transport through plant aerenchyma was the dominant transport mechanism, as ^{12}C-CH_4 has higher translation velocity which results in CH_4 emitted having more negative δ^{13}C-CH_4 values relative to the CH_4 in the pore water (Hornibrook, 2009; Marushchak et al., 2016; McCalley et al., 2014). During the winter, when peat temperature was low, the data was mostly above the 1:1 line, indicating CH_4 transport to be dominated by diffusion through peat matrix, where ^{12}C-CH_4 was preferentially consumed leaving the residual CH_4 to be enriched in ^{13}C-CH_4 (Larmola et al., 2010). During the spring and autumn, the data points were found near the 1:1 line, both above and below it, indicating the transition between the domination of diffusion through peat matrix in winter and the domination of plant transport in summer. Although LAI_{sedge} in the spring and autumn were only ca. 25% compared to that in the peak GS (Figure 2c), plant transport can be an important mechanism due to the highly efficient transport through senesced plants (Jentzsch et al., 2024).

Table 1
List of Mean and Range of $\delta^{13}C$ Values of Emitted Methane Measured From Multiple Northern Mires Including the Current Study

	Latitude	Longitude	$\delta^{13}C$ mean (‰)	$\delta^{13}C$ range (‰)	Reference
Atmospheric inversion	–	–	−60	–	Houweling et al. (2000) and Monteil et al. (2011)
Siikaneva fen	61°49.961′N	24°11.567′E	−72.0	−78.2 to −67.0	This study
Mycklemossen	58°21′N	12°10′E	−79.3	−82.0 to −77.0	Rinne et al. (2022) (based on NBLA)
Sodankylä	67°22.120′N	26°39.240′E	−72.0	−78.1 to −69.2	Fisher et al. (2017)
Lompolojänkkä	67°59.830′N	24°12.550′E	−72.0	−72.3 to −68.0	Fisher et al. (2017)
Kaamanen	69°08.430′N	27°16.190′E	−71.2	−74.0 to −68.0	Fisher et al. (2017)
Stordalen	68°21.350′N	19°02.950′E	−69.2	−69.8 to −68.6	Fisher et al. (2017)
Lompolojänkkä	67°59.832′N	24°12.551′E	−67.3	−68.8 to −64.9	Sriskantharajah et al. (2012)
Stordalen (*Sphagnum* site)	68°21′N	18°49′E	−79.6	−85.0 to −70.0	McCalley et al. (2014)
Stordalen (*Eriophorum* site)	68°21′N	18°49′E	−66.3	−74.0 to −60.0	McCalley et al. (2014)
Siikaneva bog	61°50.198′N	24°10.133′E	−75.2	−76.0 to −72.0	Jentzsch et al. (2024)
Cors Caron	52°15.400′N	03° 55.000′W	−86.6	−95.3 to −81.5	Hornibrook and Bowes (2007)
Crymlyn Bog	51°38.183′N	03°53.300′W	−67.2	−72.6 to −60.3	Hornibrook and Bowes (2007)

Note. $\delta^{13}C$ value of emitted methane commonly used in atmospheric inversions is also reported for comparison.

There is a lack of year-round paired data on $\delta^{13}C$ in emitted CH_4 and in pore water CH_4 collected in situ from boreal mires. A recent study by Jentzsch et al. (2024) is one of the rare efforts of this kind which investigated the relationship between the $\delta^{13}C$ values of emitted and pore water CH_4 over spring, summer, and autumn at the Siikaneva bog, located 1 km from the Siikaneva fen (current study site). Their study found that emitted CH_4 was more depleted in ^{13}C than pore water CH_4 in the full vegetation plot (including vascular plants and sphagnum), while emitted CH_4 was more ^{13}C enriched in the bare peat plot. This is consistent with our results showing that plant-mediated CH_4 transport leads to lower $\delta^{13}C$ values in emitted CH_4 (Figure 4c). Jentzsch et al. (2024) highlighted the effects of spatial (microtopographic) variation on $\delta^{13}C$-CH_4 values in northern mires, providing a complementary perspective to the temporal (seasonal) variation investigated in the current study. Unlike in our study, the $\delta^{13}C$-CH_4 profiles (0–50 cm) remained largely unchanged from summer to autumn, with higher values at the surface. However, due to the limited sampling frequency (seven field campaigns over one and a half years), it is difficult to determine whether CH_4 production and oxidation in the bog are relatively stable compared to the fen or if the temporal dynamics were simply obscured by the discrete sampling. Nevertheless, the distinctions between fens and bogs, as well as the resulting $\delta^{13}C$-CH_4 isotope signatures for each wetland, may not be as clear-cut as commonly believed.

Last but not least, the measured $\delta^{13}C$ in emitted methane from Siikaneva and a number of other northern mires is systematically lower than the value used in atmospheric inversion studies and source apportionment (Table 1). This is likely to lead to a considerable bias in the estimates of the contribution of northern mires in the global and regional methane emission. Furthermore, the possible seasonality of the $\delta^{13}C$ in emitted methane may further influence the seasonal inversion estimates. Thus, we recommend updating the mire $\delta^{13}C$-CH_4 signatures in the methane inventories based on reviewing data from ground measurements.

5. Conclusions

Our unique year-round high temporal resolution data set of in situ ^{13}C in dissolved CH_4 in the peat profile and in emitted CH_4 revealed the seasonally dynamic nature of methane processes in boreal mire. The generally positive correlations between ^{13}C-CH_4 and CH_4 concentrations suggest the dominance of CH_4 production in controlling the dissolved CH_4 levels over oxidation in boreal mires, except in winter. The hysteresis-like characteristics found in these relationships further indicated time-lag between the variables controlling the methane production, the peat temperature, and substrate availability.

Interestingly, the profiles of ^{13}C-CH_4 in peat water show distinctly different characteristics between winter and summer, with the former resembling profiles usually found in bogs and the latter resembling what has been

observed in fens. Although we only have data from one minerotrophic mire, our results suggest that the distinction between fens and bogs may not be as clear-cut as is commonly accepted. Seasonal variation may indeed play an important role in the biogeochemical processes of boreal mires. Analyses of the differences between ^{13}C in pore water and that in emitted methane indicated the dominance of plant-mediated methane transport in summer, the dominance of methane transport by diffusion through the peat matrix in winter, and a gradual transition of transport pathways in the spring and autumn. Besides our data also indicated the rarely studied CH_4 oxidation (at the snow-peat interface) in winter.

Boreal mires are significant natural sources of CH_4. Our comprehensive data set revealed a full annual cycle of methane dynamics along the peat profile-atmosphere continuum in a typical boreal mire. We investigated the interplay of the co-occurring processes in relation to the seasonal variation of climatic conditions, which are currently and will continue to change in the context of global warming. Such insights into methane processes, gained through continuous monitoring using novel isotope methods as in the present study, are of paramount importance for a better mechanistic understanding of wetland methane emissions and will lead to a more accurate methane emission prediction by land surface models.

Importantly, the in situ $\delta^{13}C$ value in emitted CH_4 observed in Siikaneva and a number of other northern mires systems deviates systematically from the values used in atmospheric inversions likely leading to a considerable bias in methane source apportionment.

Appendix A

Figure A1.

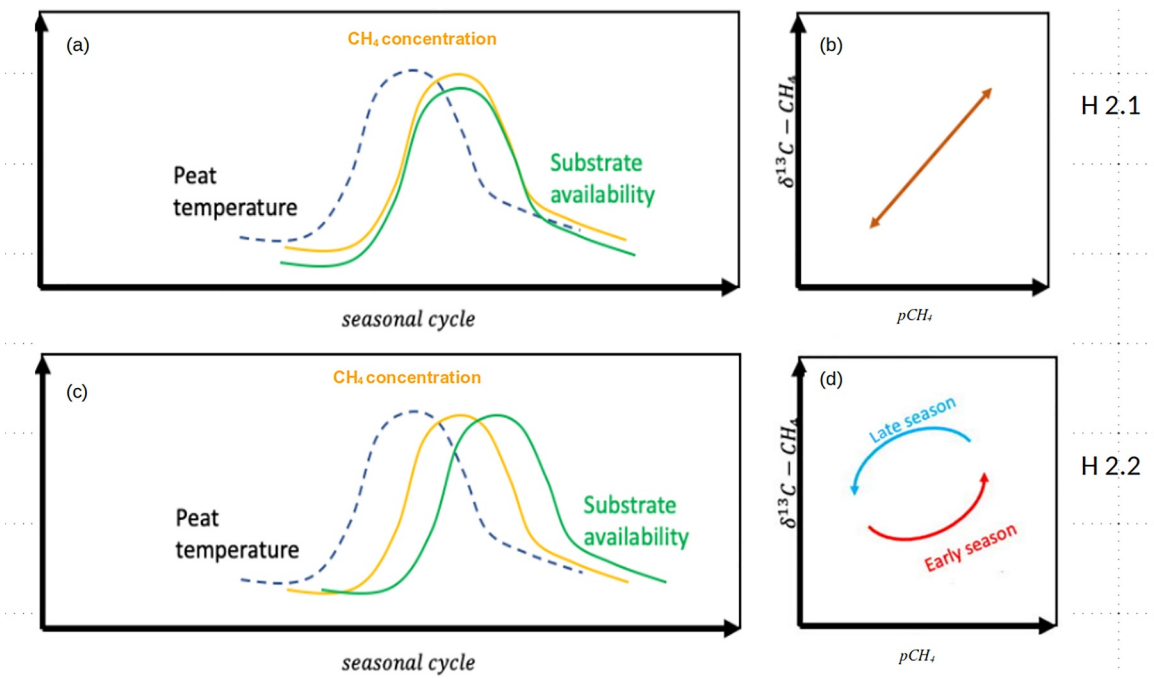

Figure A1. Hypothetical relationships between seasonal variations of environmental controls (peat temperature and substrate availability) and CH_4 concentration in the pore water (pCH_4) and resulting relations between pore water $\delta^{13}C$-CH_4 and pCH_4 (modified from Rinne et al. (2018)). In H2.1, we assume the temporal variation of pCH_4 is driven by the temporal variations of both soil temperature and substrate availability, and variation of substrate availability coincide with that of pCH_4 (a), so that pCH_4 and $\delta^{13}C$-CH_4 of pore water are positively correlated (b). In H2.2, we assume that temporal variation of pCH_4 is driven by the temporal variations of both soil temperature and substrate availability, and there is significant time-lags between the variations of substrate availability and pCH_4 (c), so that there is a hysteresis-like behavior in the relationship between pCH_4 and $\delta^{13}C$-CH_4 of pore water (d).

Table B1
Examples of Mixing Ratio (c_s) and $\delta^{13}C$-CH_4 Value ($\delta^{13}C_s$) in the Diffusion Tube, Calculated Using Measured Mixing Ratio (c_m) and $\delta^{13}C$-CH_4 Value ($\delta^{13}C_m$) and Assumed Mixing Ratio (c_m) and $\delta^{13}C$-CH_4 Value ($\delta^{13}C_d$) in the Dilution Air

c_d (ppm)	c_m (ppm)	$\delta^{13}C_d$ (‰)	$\delta^{13}C_m$ (‰)	c_s (ppm)	$\delta^{13}C_s$ (‰)
2	500	−50.00	−80.00	49,800	−80.12
3	500	−50.00	−80.00	49,700	−80.18
4	500	−50.00	−80.00	49,600	−80.24
2	100	−50.00	−80.00	9,802	−80.61
3	100	−50.00	−80.00	9,703	−80.92
4	100	−50.00	−80.00	9,604	−81.24
2	30	−50.00	−80.00	2,802	−82.12
3	30	−50.00	−80.00	2,703	−83.30
4	30	−50.00	−80.00	2,604	−84.56
2	500	−60.00	−80.00	49,800	−80.08
2	500	−70.00	−80.00	49,700	−80.04
2	100	−60.00	−80.00	9,802	−80.40
2	100	−70.00	−80.00	9,802	−80.20

Appendix B

The sample air from soil diffusion tubes was diluted with ambient air by 1:99 ratio to avoid exceedance of the operational range of Picarro G2201-i. The CH_4 mixing ratio in the diffusion tube, c_s, can be calculated by

$$\chi_s = \frac{(V_s + V_d)\chi_m - V_d\chi_d}{V_s}, \quad \text{(B1)}$$

where c_m is the CH_4 mixing ratio measured by the CRDS and c_d is the CH_4 mixing ratio in the air used for the dilution. V_s and V_d are the relative volumes of the sample (1) and dilution gas (99). The $\delta^{13}C$-CH_4 in the diffusion tube, $\delta^{13}C_s$, can be calculated by

$$\delta^{13}C_s = \frac{(\chi_s V_s + \chi_d V_d)\delta^{13}C_m - \chi_d V_d \delta^{13}C_d}{\chi_m(V_d + V_s) - \chi_d V_d}, \quad \text{(B2)}$$

where $\delta^{13}C_m$ is the measured d^{13}C-CH_4 value, and $\delta^{13}C_d$ is δ^{13}C-CH_4 value in dilution air. This formulation is mathematically identical that presented by Post (2002).

With these equations we also tested the sensitivity of the calculated c_s and $\delta^{13}C_s$ on the CH_4 mixing ratios and δ^{13}C-CH_4 in the dilution air. Examples are given in Table B1. The highest nighttime average mixing ratios over three-hour measurement periods were somewhat over 3 ppm. As can be seen, only in the case of extremely low measured CH_4 mixing ratio (30 ppm) will the difference of 1 ppm in the assumed CH_4 mixing ratio in the dilution air cause a difference of more than 1‰ units in the $\delta^{13}C_s$. For the measured mixing ratios more typical in the anaerobic peat layers below 20–30 cm of depth, the uncertainty due to the dilution air causes uncertainty of well below 1‰ units to $\delta^{13}C_s$. These uncertainties are minor compared to the observed variations in the δ^{13}C-CH_4 both in depth and during the annual cycle.

Conflict of Interest

The authors declare no conflicts of interest relevant to this study.

Data Availability Statement

The meteorological and soil data (https://doi.org/10.23729/0766621e-99bf-42f2-ad55-889cdb08b66a) and methane flux data (https://doi.org/10.23729/bcc98726-ead8-45d4-ac39-1e4b1bf5e243) from the Siikaneva site during the study period are accessible via the Finnish metadata catalog Etsin. CH_4 concentration in the pore water, δ^{13}C-CH_4 in the pore water and in emitted CH_4 as well as leaf area index of sedges can be found in Zenodo (https://zenodo.org/records/17116840). Other data are available on request from the corresponding author.

Acknowledgments
We thank Pavel Alekseychik for the hard work in installing the sample tubes into peat, Elisa Männistö for the vegetation analysis of leaf area index of the sedges, Üllar Rannik for the concentration and flux footprint analysis, and Pasi Jalkanen for the aerial photo of the Siikeneva mire. We thank the reviewers for their constructive and detailed comments. This study has been funded by the Research Council of Finland (332953) and the Research Council project 330840 and 371040. This research has been supported by the "Greenhouse Gas Fluxes and Earth System Feedbacks" (GreenFeedBack) project from the European Union's Horizon Europe Framework Programme for Research and Innovation (Project 101056921) funded by the European Union and RESPEAT (341753). This study has also been supported by ICOS-Finland by University of Helsinki, Atmosphere and Climate Competence Centre (ACCC) to University of Helsinki and University of Eastern Finland. Open access publishing facilitated by Helsingin yliopisto, as part of the Wiley - FinELib agreement.

References

Chang, K. Y., Riley, W. J., Crill, P. M., Grant, R. F., & Saleska, S. R. (2020). Hysteretic temperature sensitivity of wetland CH_4 fluxes explained by substrate availability and microbial activity. *Biogeosciences*, *17*(22), 5849–5860. https://doi.org/10.5194/bg-17-5849-2020

Chang, K. Y., Riley, W. J., Knox, S. H., Jackson, R. B., McNicol, G., Poulter, B., et al. (2021). Substantial hysteresis in emergent temperature sensitivity of global wetland CH_4 emissions. *Nature Communications*, *12*(1), 2266. https://doi.org/10.1038/s41467-021-22452-1

Chanton, J. P. (2005). The effect of gas transport on the isotope signature of methane in wetlands. *Organic Geochemistry*, *36*(5), 753–768. https://doi.org/10.1016/j.orggeochem.2004.10.007

Chanton, J. P., Chaser, L. C., Glaser, P., & Siegel, D. (2005). Isotopic eeffects aassociated with mmethane pproduction mechanisms. In L. B. Flanagan, J. R. Ehleringer, & D. E. Pataki (Eds.), *Stable iisotopes and bbiosphere-aatmosphere iinteractions* (pp. 85–105). Elsevier.

Ciais, P., Sabine, C., Bala, G., Bopp, L., Brovkin, V., Canadell, J., et al. (2013). Carbon and oother bbiogeochemical ccycles. In T. Stocker, D. Qin, G. Plattner, M. Tignor, S. Allen, J. Boschung, et al. (Eds.), *Climate change 2013: The physical science basis. Contribution of working group I to the fifth assessment report of the iintergovernmental ppanel on cclimate cchange* (pp. 465–570). Cambridge University Press.

Dise, N. B. (1992). Winter fluxes of methane from Minnesota peatlands. *Biogeochemistry*, *17*(2), 71–83. https://doi.org/10.1007/bf00002641

Finnish Meteorological Institute. (2024). Seasons in Finland. Retrieved from https://en.ilmatieteenlaitos.fi/seasons-in-finland

Fisher, R. E., France, J. L., Lowry, D., Lanoisellé, M., Brownlow, R., Pyle, J. A., et al. (2017). Measurement of the ^{13}C isotopic signature of methane emissions from northern European wetlands. *Global Biogeochemical Cycles*, *31*(3), 605–623. https://doi.org/10.1002/2016gb005504

Gedney, N., Cox, P. M., & Huntingford, C. (2004). Climate feedback from wetland methane emissions. *Geophysical Research Letters*, *31*(20), L20503. https://doi.org/10.1029/2004gl020919

Heiskanen, J., Brümmer, C., Buchmann, N., Calfapietra, C., Chen, H. L., Gielen, B., et al. (2022). The integrated carbon observation system in Europe. *Bulletin of the American Meteorological Society*, *103*(3), E855–E872. https://doi.org/10.1175/bams-d-19-0364.1

Heiskanen, L., Tuovinen, J. P., Räsänen, A., Virtanen, T., Juutinen, S., Lohila, A., et al. (2021). Carbon dioxide and methane exchange of a patterned subarctic fen during two contrasting growing seasons. *Biogeosciences*, *18*(3), 873–896. https://doi.org/10.5194/bg-18-873-2021

Hornibrook, E. R. C. (2009). The sstable ccarbon iisotope ccomposition of mmethane pproduced and eemitted ffrom nnorthern peatlands. In A. J. Baird, L. R. Belyea, X. Comas, A. S. Reeve, & L. D. Slater (Eds.), *Carbon ccycling in northern peatlands* (Vol. 184, pp. 187–203). https://doi.org/10.1029/2008gm000828

Hornibrook, E. R. C., & Bowes, H. L. (2007). Trophic status impacts both the magnitude and stable carbon isotope composition of methane flux from peatlands. *Geophysical Research Letters*, *34*(21), L21401. https://doi.org/10.1029/2007gl031231

Hornibrook, E. R. C., Longstaffe, F. J., & Fyfe, W. S. (1997). Spatial distribution of microbial methane production pathways in temperate zone wetland soils: Stable carbon and hydrogen isotope evidence. *Geochimica et Cosmochimica Acta*, *61*(4), 745–753. https://doi.org/10.1016/s0016-7037(96)00368-7

Houweling, S., Dentener, F., & Lelieveld, J. (2000). Simulation of preindustrial atmospheric methane to constrain the global source strength of natural wetlands. *Journal of Geophysical Research*, *105*(D13), 17243–17255. https://doi.org/10.1029/2000jd900193

Jentzsch, K., Männistö, E., Marushchak, M. E., Korrensalo, A., van Delden, L., Tuittila, E. S., et al. (2024). Shoulder season controls on methane emissions from a boreal peatland. *Biogeosciences*, *21*(16), 3761–3788. https://doi.org/10.5194/bg-21-3761-2024

Jokinen, P., Pirinen, P., Kaukoranta, J.-P., Kangas, A., Alenius, P., Eriksson, P., et al. (2021). Tilastoja Suomen ilmastosta ja merestä 1991-2020 (climatological and oceanographic statistics of Finland 1991–2020).

Keane, J. B., Toet, S., Ineson, P., Weslien, P., Stockdale, J. E., & Klemedtsson, L. (2021). Carbon ddioxide and mmethane fflux rresponse and rrecovery ffrom ddrought in a hemiboreal ombrotrophic fen. *Frontiers in Earth Science*, *8*, 562401. https://doi.org/10.3389/feart.2020.562401

Keeling, C. D. (1958). The concentration and isotopic abundance of atmospheric carbon dioxide in rural area. *Geochimica et Cosmochimica Acta*, *13*(4), 322–334. https://doi.org/10.1016/0016-7037(58)90033-4

Knorr, K. H., Glaser, B., & Blodau, C. (2008). Fluxes and C-13 isotopic composition of dissolved carbon and pathways of methanogenesis in a fen soil exposed to experimental drought. *Biogeosciences*, *5*(5), 1457–1473. https://doi.org/10.5194/bg-5-1457-2008

Korrensalo, A., Alekseychik, P., Hajek, T., Rinne, J., Vesala, T., Mehtatalo, L., et al. (2017). Species-specific temporal variation in photosynthesis as a moderator of peatland carbon sequestration. *Biogeosciences*, *14*(2), 257–269. https://doi.org/10.5194/bg-14-257-2017

Korrensalo, A., Kettunen, L., Laiho, R., Alekseychik, P., Vesala, T., Mammarella, I., & Tuittila, E. S. (2018). Boreal bog plant communities along a water table gradient differ in their standing biomass but not their biomass production. *Journal of Vegetation Science*, *29*(2), 136–146. https://doi.org/10.1111/jvs.12602

Kuhn, M. A., Varner, R. K., McCalley, C. K., Perryman, C. R., Aurela, M., Burke, S. A., et al. (2024). Controls on sstable mmethane iisotope vvalues in nnorthern peatlands and ppotential sshifts in vvalues uunder permafrost thaw sscenarios. *Journal of Geophysical Research: Biogeosciences*, *129*(7). e2023JG007837. https://doi.org/10.1029/2023JG007837

Lai, D. Y. F. (2009). Methane ddynamics in nnorthern peatlands: A rreview. *Pedosphere*, *19*(4), 409–421. https://doi.org/10.1016/s1002-0160(09)00003-4

Larmola, T., Tuittila, E. S., Tiirola, M., Nykanen, H., Martikainen, P. J., Yrjala, K., et al. (2010). The role of Sphagnum mosses in the methane cycling of a boreal mire. *Ecology*, *91*(8), 2356–2365. https://doi.org/10.1890/09-1343.1

Marushchak, M. E., Friborg, T., Biasi, C., Herbst, M., Johansson, T., Kiepe, I., et al. (2016). Methane dynamics in the subarctic tundra: Combining stable isotope analyses, plot- and ecosystem-scale flux measurements. *Biogeosciences*, *13*(2), 597–608. https://doi.org/10.5194/bg-13-597-2016

Mathijssen, P. J. H., Valiranta, M., Korrensalo, A., Alekseychik, P., Vesala, T., Rinne, J., & Tuittila, E. S. (2016). Reconstruction of Holocene carbon dynamics in a large boreal peatland complex, southern Finland. *Quaternary Science Reviews*, *142*, 1–15. https://doi.org/10.1016/j.quascirev.2016.04.013

McCalley, C. K., Woodcroft, B. J., Hodgkins, S. B., Wehr, R. A., Kim, E. H., Mondav, R., et al. (2014). Methane dynamics regulated by microbial community response to permafrost thaw. *Nature*, *514*(7523), 478–481. https://doi.org/10.1038/nature13798

Monteil, G., Houweling, S., Dlugockenky, E. J., Maenhout, G., Vaughn, B. H., White, J. W. C., & Rockmann, T. (2011). Interpreting methane variations in the past two decades using measurements of CH_4 mixing ratio and isotopic composition. *Atmospheric Chemistry and Physics*, *11*(17), 9141–9153. https://doi.org/10.5194/acp-11-9141-2011

Nemitz, E., Mammarella, I., Ibrom, A., Aurela, M., Burba, G. G., Dengel, S., et al. (2018). Standardisation of eddy-covariance flux measurements of methane and nitrous oxide. *International Agrophysics*, *32*(4), 517–549. https://doi.org/10.1515/intag-2017-0042

Peltola, O., Vesala, T., Gao, Y., Räty, O., Alekseychik, P., Aurela, M., et al. (2019). Monthly gridded data product of northern wetland methane emissions based on upscaling eddy covariance observations. *Earth System Science Data*, *11*(3), 1263–1289. https://doi.org/10.5194/essd-11-1263-2019

Perryman, C. R., McCalley, C. K., Shorter, J. H., Perry, A. L., White, N., Dziurzynski, A., & Varner, R. K. (2024). Effect of drought and heavy precipitation on CH_4 emissions and $\delta^{13}C$-CH_4 in a northern temperate peatland. *Ecosystems*, *27*(1), 1–18. https://doi.org/10.1007/s10021-023-00868-8

Popp, T. J., Chanton, J. P., Whiting, G. J., & Grant, N. (1999). Methane stable isotope distribution at a Carex dominated fen in north central Alberta. *Global Biogeochemical Cycles*, *13*(4), 1063–1077. https://doi.org/10.1029/1999gb900060

Post, D. (2002). Using stable isotopes to estimate trophic position: Models, methods, and assumptions. *Ecology*, *83*(3), 703–718. https://doi.org/10.1890/0012-9658(2002)083[0703:USITET]2.0.CO;2

Quay, P. D., King, S. L., Lansdown, J. M., & Wilbur, D. O. (1988). Isotopic composition of methane release from wetlands: Implications for the increase in atmospheric methane. *Global Biogeochemical Cycles*, *2*(4), 385–397. https://doi.org/10.1029/GB002i004p00385

Rannik, Ü., Markkanen, T., Raittila, J., Hari, P., & Vesala, T. (2003). Turbulence statistics inside and over forest: Influence on footprint prediction. *Boundary-Layer Meteorology*, *109*(2), 163–189. https://doi.org/10.1023/a:1025404923169

Rinne, J., Lakomiec, P., Vestin, P., White, J. D., Weslien, P., Kelly, J., et al. (2022). Spatial and temporal variation in $\delta^{13}C$ values of methane emitted from a hemiboreal mire: Methanogenesis, methanotrophy, and hysteresis. *Biogeosciences*, *19*(17), 4331–4349. https://doi.org/10.5194/bg-19-4331-2022

Rinne, J., Riutta, T., Pihlatie, M., Aurela, M., Haapanala, S., Tuovinen, J. P., et al. (2007). Annual cycle of methane emission from a boreal fen measured by the eddy covariance technique. *Tellus Series B Chemical and Physical Meteorology*, *59*(3), 449–457. https://doi.org/10.1111/j.1600-0889.2007.00261.x

Rinne, J., Tuittila, E. S., Peltola, O., Li, X. F., Raivonen, M., Alekseychik, P., et al. (2018). Temporal variation of ecosystem scale methane emission from a boreal fen in relation to temperature, water table position, and carbon dioxide fluxes. *Global Biogeochemical Cycles*, *32*(7), 1087–1106. https://doi.org/10.1029/2017gb005747

Riutta, T., Laine, J., Aurela, M., Rinne, J., Vesala, T., Laurila, T., et al. (2007). Spatial variation in plant community functions regulates carbon gas dynamics in a boreal fen ecosystem. *Tellus Series B Chemical and Physical Meteorology*, *59*(5), 838–852. https://doi.org/10.1111/j.1600-0889.2007.00302.x

Sabrekov, A. F., Semenov, M. V., Terentieva, I. E., Krasnov, G. S., Kharitonov, S. L., Glagolev, M. V., & Litti, Y. V. (2024). Anaerobic methane oxidation is quantitatively important in deeper peat layers of boreal peatlands: Evidence from anaerobic incubations, in situ stable isotopes depth profiles, and microbial communities. *Science of the Total Environment*, *916*, 170213. https://doi.org/10.1016/j.scitotenv.2024.170213

Schulz, S., Matsuyama, H., & Conrad, R. (1997). Temperature dependence of methane production from different precursors in a profundal sediment (Lake Constance). *FEMS Microbiology Ecology*, *22*(3), 207–213. https://doi.org/10.1016/s0168-6496(96)00091-8

Shoemaker, J. K., & Schrag, D. P. (2010). Subsurface characterization of methane production and oxidation from a New Hampshire wetland. *Geobiology*, *8*(3), 234–243. https://doi.org/10.1111/j.1472-4669.2010.00239.x

Sriskantharajah, S., Fisher, R. E., Lowry, D., Aalto, T., Hatakka, J., Aurela, M., et al. (2012). Stable carbon isotope signatures of methane from a Finnish subarctic wetland. *Tellus Series B Chemical and Physical Meteorology*, *64*(1), 18818. https://doi.org/10.3402/tellusb.v64i0.18818

Turetsky, M. R., Kotowska, A., Bubier, J., Dise, N. B., Crill, P., Hornibrook, E. R. C., et al. (2014). A synthesis of methane emissions from 71 northern, temperate, and subtropical wetlands. *Global Change Biology*, *20*(7), 2183–2197. https://doi.org/10.1111/gcb.12580

Wania, R., Melton, J. R., Hodson, E. L., Poulter, B., Ringeval, B., Spahni, R., et al. (2013). Present state of global wetland extent and wetland methane modelling: Methodology of a model inter-comparison project (WETCHIMP). *Geoscientific Model Development*, *6*(3), 617–641. https://doi.org/10.5194/gmd-6-617-2013

Whiticar, M. J. (1999). Carbon and hydrogen isotope systematics of bacterial formation and oxidation of methane. *Chemical Geology*, *161*(1–3), 291–314. https://doi.org/10.1016/s0009-2541(99)00092-3

Whiticar, M. J., Faber, E., & Schoell, M. (1986). Biogenic methane formation in marine and fresh-water environments-CO_2 reduction vs acetate fermentation isotope evidence. *Geochimica et Cosmochimica Acta*, *50*(5), 693–709. https://doi.org/10.1016/0016-7037(86)90346-7

Xu, X. F., Yuan, F. M., Hanson, P. J., Wullschleger, S. D., Thornton, P. E., Riley, W. J., et al. (2016). Reviews and syntheses: Four decades of modeling methane cycling in terrestrial ecosystems. *Biogeosciences*, *13*(12), 3735–3755. https://doi.org/10.5194/bg-13-3735-2016

Yvon-Durocher, G., Allen, A. P., Bastviken, D., Conrad, R., Gudasz, C., St-Pierre, A., et al. (2014). Methane fluxes show consistent temperature dependence across microbial to ecosystem scales. *Nature*, *507*(7493), 488–491. https://doi.org/10.1038/nature13164

Zhang, Z., Poulter, B., Feldman, A. F., Ying, Q., Ciais, P., Peng, S. S., & Li, X. (2023). Recent intensification of wetland methane feedback. *Nature Climate Change*, *13*(5), 430–433. https://doi.org/10.1038/s41558-023-01629-0